Geol. Mag. **137** (6), 2000, pp. 667–685. *Printed in the United Kingdom* © 2000 Cambridge University Press

Thrust dissection control of deep-water clastic dispersal patterns in the Klematia–Paramythia foreland basin, western Greece

PAVLOS AVRAMIDIS*, ABRAHAM ZELILIDIS & NIKOLAOS KONTOPOULOS

University of Patras, Department of Geology, 26500 Patras, Greece

(*Received* 16 June 1999; *revised version received* 23 June 2000; *accepted* 2 August 2000)

Abstract – The Klematia–Paramythia basin is an internal part of the middle Ionian zone of the Hellenide orogen in western Greece. It consists of Middle Eocene to Late Miocene turbidites, up to 3300 m thick, which were deposited in a series of submarine fans. Field studies suggest that the configuration and the depositional environments of the basin were affected by two tectonic phases. During the first tectonic phase, in Middle Eocene to Late Oligocene times, a foreland basin was formed west of the Pindos Thrust front. During the second tectonic phase, in the Early Miocene, the Ionian zone (a part of the foreland basin) was subdivided by internal thrusting into three sub-basins (internal, middle and external) and changed to a complex type foreland basin. Comparison of the type and facies associations of the turbidite deposits that accumulated within the basin suggests that these two tectonic phases had a significant effect on sedimentary dispersal patterns. During the first tectonic phase in the Klematia–Paramythia basin (when it was part of the foreland basin), fine-grained turbidites, up to 1050 m thick, accumulated on the distal part of a submarine fan. The lower part (900 m thick) of these deposits consists of thin to thick interbedded sandstone/mudstone beds which are interpreted as lobes and lobe-fringe (outer-fan) deposits. The upper parts (150 m thick) of these deposits are composed of very thin to thin siltstone/mudstone beds, representing a basin plain environment. During the second tectonic phase, sediments up to 2260 m thick were deposited in the Klematia–Paramythia basin. These deposits are interpreted as lobes and lobe-fringe (outer-fan) fine-grained turbidites in the central part of the basin, channel and interchannel deposits (inner-fan) in some areas of the periphery of the basin, and shelf deposits in the northern and southern terminations of the basin.

1. Introduction

Early sedimentation in foreland basins is commonly dominated by marine turbidite deposits. Turbidite foreland basin fills have been described by Mutti (1985), Ricci Lucchi (1986), Hiscott, Pickering & Beeden (1986) and others. A large number of foreland basins with petroleum production from submarine fans have been reviewed by Weimer & Link (1991).

Examples of elongated foreland basins which have been filled mostly by turbidite deposits are the Oligocene to Recent basins of the northern Apennines (Ricci Lucchi, 1986; Ori, Roveri & Vannoni, 1986) that continue into the Ionian Sea. The Padan and Adriatic basins are examples of complex foreland basins with internal thrusts. These basins can be created either stepwise or at the same time, splitting into minor basins with subequal or different sizes (Ricci Lucchi, 1986).

Attempts to classify submarine fans have been made by Normark (1970), Walker & Mutti (1973), Mutti & Ricci Lucchi (1975), Ricci Lucchi (1975), Nelson & Nilsen (1984), Mutti & Normark (1987), Shanmugam & Moiola (1988), Ghibaudo (1992), Reading & Richards (1994) and Shanmugam (1997). According to Ricci Lucchi (1975), there are four major elements that characterize the development of a submarine fan: (a) inner fan, (b) middle fan, (c) outer fan and (d) basin plain. The inner fan consists of channel-fill, interchannel, levee and channel mouth bar deposits, representing the proximal part of the submarine fan. The middle fan is characterized by features from both the inner and outer fans. The outer fan consists of lobes and lobe-fringe deposits representing the transition between the proximal and the more distal part of the fan. The basin plain consists of the finest material of the fan (mudstone–siltstone) and represents the most distal parts. Moreover, seven facies were introduced by Walker & Mutti (1973): A–G, which are associated with the subenvironments of the submarine fan and which have also been used by Walker (1978) and Shanmugam & Moiola (1985) to correlate these facies to subenvironments. Mutti & Normark (1987) distinguished four main types of channel-fill deposits observed in ancient turbidites: type (a) representing erosional channels; type (b1) representing depositional channels with thick-bedded and coarse-grained amalgamated axial facies; type (b2) representing depositional channels, filled with alternating sandstone and mudstone beds, and type (c) to which are referred types of channels with mixed features of the above

*Author for correspondence: P.Avramidis@upatras.gr

https://doi.org/10.1017/S0016756800004684 Published online by Cambridge University Press

channel types. Mutti (1985) classified turbidite systems in relation to their depositional sequences and to the relative sea-level variations into three main system types: I, II and III.

In the last twenty years, a number of papers have been written about the re-evaluation and re-interpretation of the submarine fan models and the comparison between ancient and modern submarine fan systems (Shanmugam, Damuth, & Moiola, 1985; Stow, Reading & Collinson, 1996; Shanmugam, 1997; Shanmugam, 2000; Bouma, 2000; Stow & Mayall, 2000). Although there are critical papers about the problems associated with deep-water processes and related facies models (see detailed review in Shanmugam, 2000), the previous classification schemes of Mutti & Ricci Lucchi (1972, 1975), Walker & Mutti (1973), Walker (1978) and Mutti (1979) are widely accepted and are incorporated in new proposed models and applications (Pickering *et al.* 1986; Pickering, Hiscott & Hein, 1989; Weimer & Link, 1991; Ghibaudo, 1992; Boiano, 1997).

The study area is part of the external Hellenides and belongs to the Pindos foreland, an example of Tertiary turbiditic foreland basin fill, segmented during its evolution by thrusting and strike-slip motions. The scope of this paper is to describe and interpret the subenvironments of submarine fans in the Klematia–Paramythia basin, and to classify the turbidite facies and facies associations (Mutti & Ricci Lucchi, 1975; Mutti, 1977; Mutti, 1985). In the framework of basin analysis, an attempt is made to correlate the depositional environments of the study basin with the tectonic regime and the evolution of the external Hellenides, the telescoped remnants of a former (Mesozoic) passive continental margin (Underhill, 1989).

2. Geological setting

The Klematia–Paramythia basin is located in Epirus, western Greece, between latitude 39°24′ and 39°45′N and longitude 20°30′ and 20°46′W. It is an elongated basin with a northwest–southeast trend and belongs to the middle Ionian zone. The Ionian zone is subdivided from east to west into the internal, middle and external Ionian zones (IGSR & IFP, 1966) (Fig. 1). The basin trend is parallel to the external Hellenides, which consist, from east to west, of the Pindos, Gavrovo, Ionian and Pre-Apulian geotectonic zones (Aubouin, 1965). The external Hellenides represent parts of the Apulian plate which were separated from the Pelagonian microplate by the Pindos ocean (Robertson *et al.* 1991; Jones, De Wever & Robertson, 1992). There are two major thrusts, the Pindos and Ionian thrusts, which are situated in the eastern and western margins of the Pindos foreland, respectively, and two minor thrusts (the internal and middle Ionian thrusts) that are restricted to the basin (Fig. 1).

As the deformation of the external Hellenides migrated westwards, flysch deposits derived from the Pindos mountains accumulated on the footwall of the Pindos thrust. During this migration of the external Hellenides, the Gavrovo and Ionian zones acted as a foreland basin, as first proposed by Underhill (J. R. Underhill, unpub. Ph.D. thesis, Univ. Wales Cardiff, 1985), Brooks *et al.* (1988), Underhill (1989) and later by Clews (1989), Alexander, Nichols & Leigh (1990) and Avramidis (P. Avramidis, unpub. Ph.D. thesis, Univ. Patras, 1999). The flysch deposits in some places conformably overlie Eocene limestone, while there are places where their contact is marked by an uncomformity. The onset of flysch sedimentation in the Pindos foreland is a controversial point as there are studies with different definitions of sediment ages. IGSR & IFP (1966) proposed that the onset of flysch sedimentation took place in Late Eocene time, while Fleury (1980), Leigh (S. Leigh, unpub. Ph.D. thesis, Univ. Wales Cardiff, 1991), Wilpshaar (1995) and Bellas (1997) proposed an Early Oligocene age. In contrast to the above studies, B.P. (1971) proposed an Early to Middle Miocene age for the onset of flysch sedimentation. Alexander, Nichols & Leigh (1990) suggested that the flysch sediments in the Gavrovo and internal Ionian zones were derived from the same genetic system, as the result of the activity on the Pindos thrust.

The flysch of the Ionian zone has been interpreted first by Piper, Panagos & Pe (1978) as parts of a submarine fan. Sedimentological data indicate that the turbidites were derived from the east and the source material of this submarine fan was the Pindos front (Piper, Panagos & Pe, 1978; Fleury, 1980; Clews, 1989; Wilpshaar, 1995; Faupl, Pavlopoulos & Migiros, 1998).

The division of the Ionian zone into internal, middle and external basins took place during Late Oligocene to Early Miocene times (IGSR & IFP, 1966). Two hypotheses have been proposed related to the time of thrust activity. The first hypothesis has been supported by Dercourt & Thiebault (1979), Fleury (1980) and Clews (1989) and suggests that the displacement of the Pindos thrust had begun by the Middle Eocene and remained active until Oligocene times when the Gavrovo thrust was activated. According to this hypothesis, the Ionian thrust was activated during Early to Late Miocene times. The second hypothesis has been proposed by Wilpshaar (1995) and suggests that during the Early to Late Oligocene, the major Ionian thrust and the internal thrusts of the Ionian zone had contemporaneous activity with the Pindos thrust, during the westward progradation of the external Hellenides. According to this hypothesis, the Pindos and internal Ionian zones emerged, whereas the external and middle Ionian zones were acting as a piggy-back basin, due to Ionian thrust.

The Klematia–Paramythia basin, as part of the middle Ionian zone, consists of thick turbidite sequences, which were deposited during the westward

https://doi.org/10.1017/S0016756800004684 Published online by Cambridge University Press

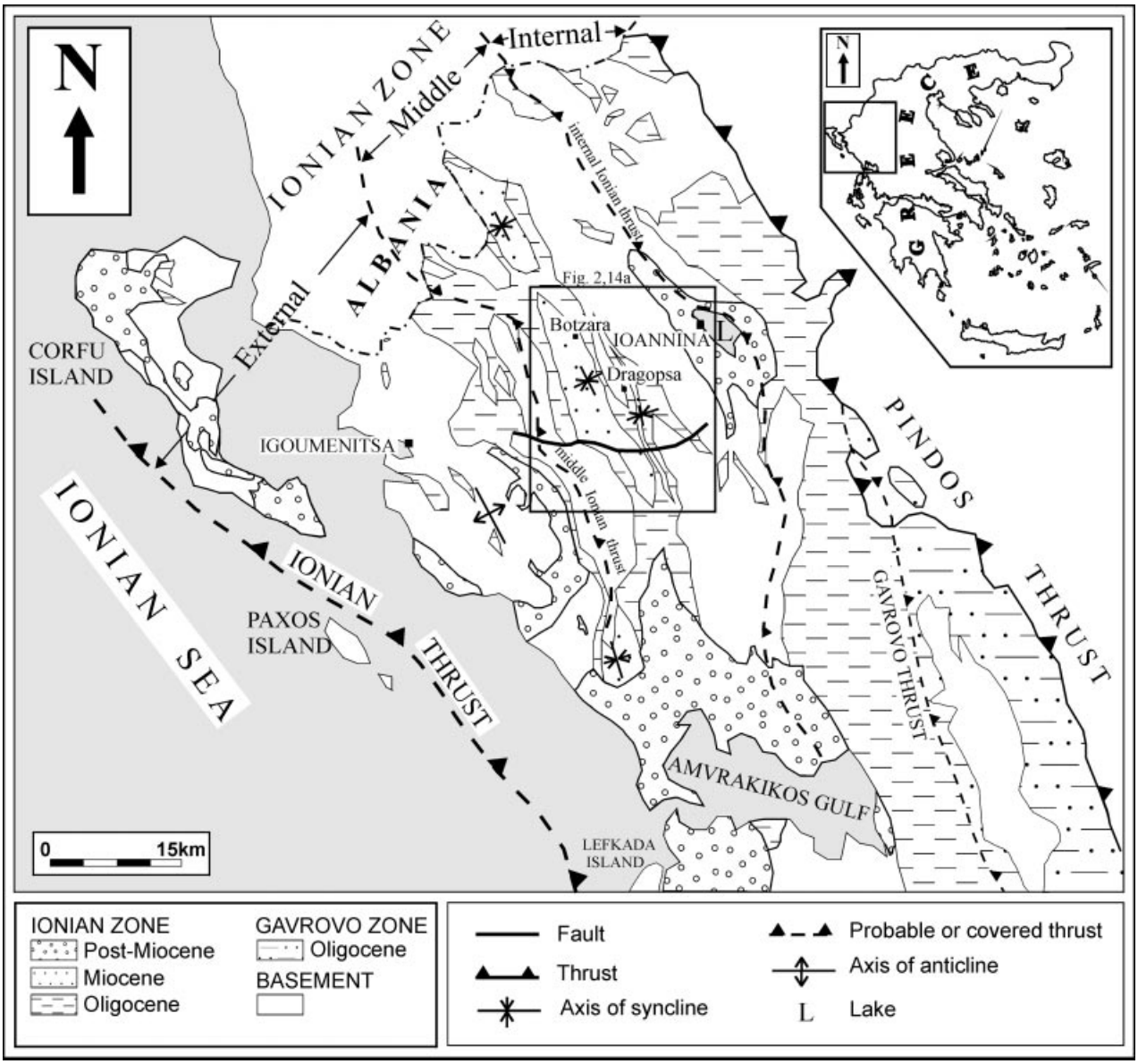


Figure 1. Simplified geological map of western Greece, showing the Ionian and Gavrovo zones (modified after IGSR & IFP, 1966) and the location of the study basin.

progradation of the external Hellenides and extend longitudinally to the axis of the Botzara syncline. Wilpshaar (1995) suggested that the turbidites of the middle Ionian zone have an Early Oligocene (Rupelian) to Early Miocene age and interpreted them as the distal part of a submarine fan. According to King, Strudy & Whitney (1993), the Klematia–Paramythia basin configuration was affected by a strike-slip fault (Agia Kyriaki fault) and by a strike-slip transpressional fault (Kourenton fault), which control the locations of the Dragopsia and Botzara synclines (Fig. 2). The Agia Kyriaki fault is a major Neogene E–W-trending left-lateral strike-slip structure. According to IGSR & IFP (1966) the Agia Kyriaki fault has been active since Liassic times, but its major activity followed the deposition of the Oligocene–Miocene turbidite deposits (Pavlides, 1996; Boccaletti *et al.* 1997; in their papers these authors refer to the Agia Kyriaki fault as the Souli fault).

Avramidis & Kontopoulos (1998), using palaeoflow indices, suggested that during Middle Eocene to Late Oligocene times the palaeoflow trends of the submarine fans were almost the same as the direction of progradation of the Pindos foreland, ENE–WSW, while during Early to Late Miocene times the trends changed, as both palaeoflow indices with NNW–SSE and ENE–WSW have been observed. Avramidis & Zelilidis (1998) recognized two different submarine fan lobe types (detached and attached lobes) and in relation to the basin evolution suggested that the detached lobes were the result of both hydrodynamic control and tectonic activity.

https://doi.org/10.1017/S0016756800004684 Published online by Cambridge University Press

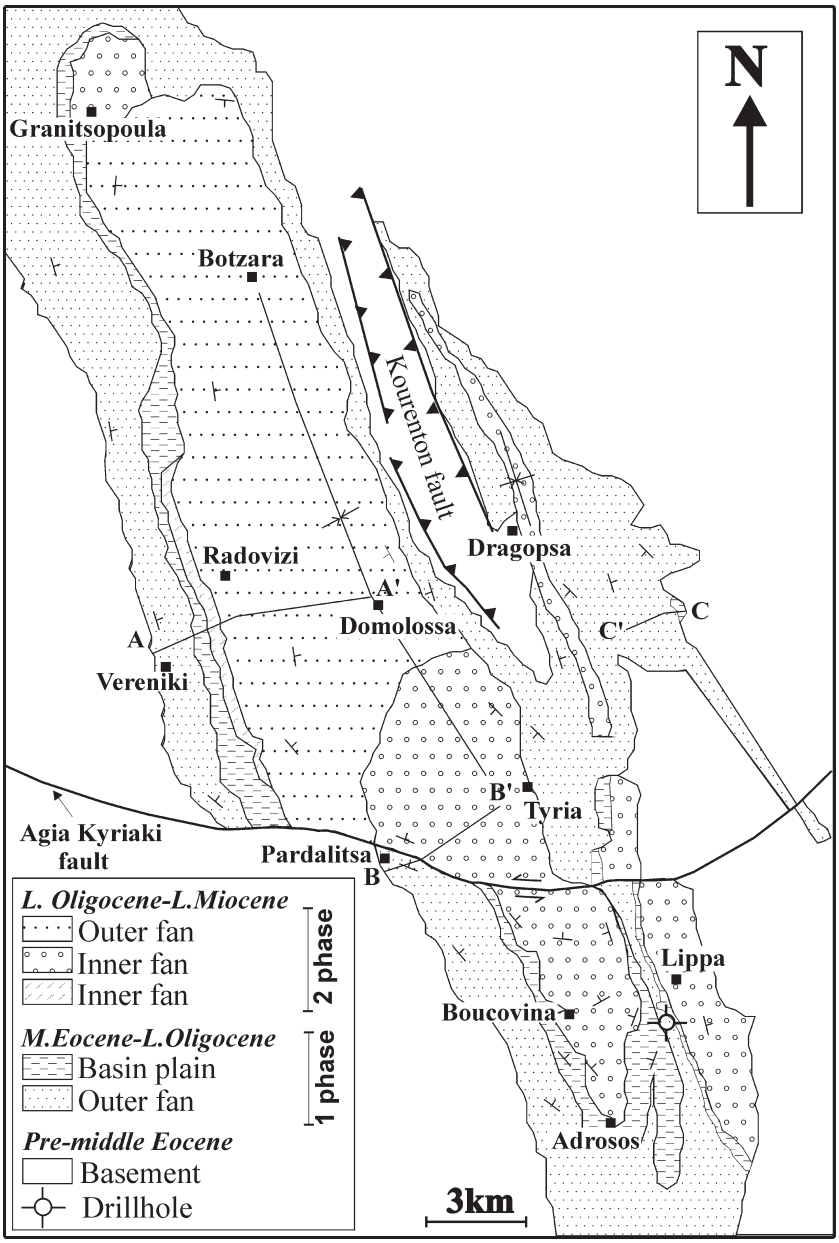


Figure 2. Geological map showing the turbidite sub-environment distribution of the Klematia–Paramythia basin and the localities of the cross-sections.

3. Depositional environments

In order to understand better the depositional setting and stratigraphic architecture, the sediments of the Klematia–Paramythia basin have been studied in three main cross-sections. The first cross-section (A–A′) is situated in the central part of the basin, the second cross-section (B–B′) in the southern part of the basin and the third (C–C′) in eastern margins of the basin (Fig. 2). The description of the turbidite successions is based on the Mutti & Normark (1987) classification of turbidite units into five hierarchical orders (1 – turbidite complex, 2 – turbidite system, 3 – turbidite stage, 4 – turbidite sub-stage and 5 – cycle). According to this hierarchy, 'turbidite complex' describes deposition affected by major breaks in sedimentation produced by long-term base-level change (due to sea-level change or tectonic activity) which generated turbidite systems stacked one on the other, producing changes in sedimentation but no significant breaks. 'Turbidite stage' refers to short-term sea-level variations and records a specific period of growth of the fan system. 'Turbidite sub-stage' describes high-frequency changes in depositional and erosional processes and is commonly stacked to form a facies association and small-scale erosion–deposition cycles composed of beds.

https://doi.org/10.1017/S0016756800004684 Published online by Cambridge University Press

3.a. Geological cross-section A–A′ (Vereniki–Domolossa turbidite complex)

Cross-section A–A′ has a total stratigraphic thickness up to 3300 m. This cross-section consists of two turbidite systems. The lower turbidite system is up to 1042 m thick and the upper system is up to 2258 m thick (Fig. 3).

3.a.1. Description

Lower turbidite system (*1042 m*). On the basis of bed thickness, the sandstone/mudstone ratio (s:m) and internal structures, three different turbidite stages have been recognized within the lower turbidite system:

(a) The lower turbidite stage (A) (388 m) comformably overlies Eocene limestone and consists of alternations between two different types of turbidite sub-stage (a and b) (Fig. 3). The thickness of the type (a) sub-stage ranges from 10 m to 50 m and the thickness of the type (b) sub-stage ranges from 10 to 95 m.

Sub-stage type (a) consist of cyclic alternations up to 7 m thick which consist of thin to medium interbedded yellowish grey calcareous sandstone and greyish mudstone (6–35 cm) with s:m ratio between 1:1 and 2:1 (Figs 3, 4). The contacts between the interbedded sandstones/mudstones are sharp, and groove and tool marks are also present at the base of the sandstone beds. The sandstones are characterized by normal grading and mostly by Tbce Bouma intervals (Bouma, 1962). The sandstone beds have a tabular shape, with some exceptions where lenticularity is observed in thicker (up to 30 cm) sandstone beds. The mudstone beds represent the Te Bouma interval and are composed of thin interbedded fissile mudstone. The alternations of these cycles are so abundant that the sub-stage type (a) is represented by units up to 50 m thick.

Sub-stage type (b) consists of cyclic alternations 5.5–8 m thick, which consist of medium to thick interbedded yellowish grey calcareous sandstone and greyish mudstone beds (12–50 cm) (Figs 3, 5). Each cycle consists of a thickening- and coarsening-upward sequence with s:m ratio of 1:2 in the lower two metres passing upwards to 5:1. The sandstone beds have a maximum thickness of 0.5 m. Bouma intervals Tabcd are present (Fig. 6). The Ta interval is observed in the thickest sandstone beds, in the upper parts of the cycle, where erosional features such as sole marks are also present.

(b) The middle turbidite stage (B) (504 m) comprises cyclic alternations up to 6–8 m thick (Fig. 3). Each cycle consists of medium to thick interbedded yellowish grey sandstone (15–75 cm) and blue to greyish mudstone beds (15–60 cm). In the lower 3 m the s:m ratio is 1:4 passing upwards to 6:1, where the sandstone beds achieve their maximum thickness of 60 cm. Bouma intervals Tbce are present. Sandstone beds thicken and coarsen upward with grain size ranging from medium to coarse. Water escape and normal grading structures are observed in sandstone beds.

(c) The upper turbidite stage (C) (150 m) consists of fissile greyish laminated interbedded mudstone beds with lateral continuity and thin to medium bedded sandstone intercalations (Figs 3, 7).

Upper turbidite system (*2258 m*): The upper turbidite system unconformably overlies the lower turbidite system and is subdivided into two turbidite stages (A and B).

(a) The lower turbidite stage (A) (86 m) consists of two sub-stages (a and b) (Fig. 3).

The lower sub-stage (a), 22 m thick, comprises fining- and thinning-upward cycles up to 5 m thick, which consist of thick greyish yellow, massive, channelized calcareous sandstone beds that pass upwards to greyish thin interbedded mudstone beds with thin to medium sandstone intercalations. The thickness of channelized sandstone beds ranges from 1.5–2.5 m, and they are characterized by the absence of Bouma sequence and the presence of tabular erosional bases.

The upper sub-stage (b), 64 m thick, consists of disturbed sediments with mudstone/sandstone clasts containing some coal, chaotic bedding and rare mollusc fragments, and characterized by slump structures and slide planes (Fig. 8).

(b) The upper turbidite stage (B) (2172 m) is composed of alternations of three different types of cycle (Fig. 3).

The first type of cycle, up to 9 m thick, consists of medium to very thick greyish yellow sandstone and thin-bedded blue-grey mudstone beds. The thicker 1.1–3.5 m sandstone beds are characterized by amalgamated Tbc Bouma intervals and by flute casts at their bases. The Tc Bouma interval is represented by convolute lamination. Sandstone beds in this type of cycle thicken and coarsen upward, with grain size ranging from fine to coarse. The s:m ratio in the lower 4 m is 1:5 passing upwards to 8:1.

The second type of cycle, up to 9.5 m thick, comprises thickening- and coarsening-upward sandstone beds and consists of thin to very thick interbedded pale yellowish calcareous sandstone and blue-grey mudstone beds with the grain size of the sandstone beds ranging from fine to coarse. The s:m ratio fluctuates between 1:5 in the lower 3.5 m, 1:2 to 1:1 in the next 2.5 m, and 5:1 to 9:1 in the upper 3.5 m. The thickest sandstone beds are, in some places, amalgamated and characterized by Tbc Bouma intervals.

The third type of cycle, up to 6 m thick, consists of thickening- and coarsening-upward calcareous sandstone beds and thin interbedded mudstones. The ratio of s:m changes from 1:4 in the lower 3 m to 1:1 and 3:1 in the upper 3 m. In the thickest sandstone beds, lenticular features are observed in some places.

Bioturbation is common in all three types of cycle and is observed in the lower 2 m of each cycle, within the mudstone beds. Burrows are horizontal and vertical,

https://doi.org/10.1017/S0016756800004684 Published online by Cambridge University Press

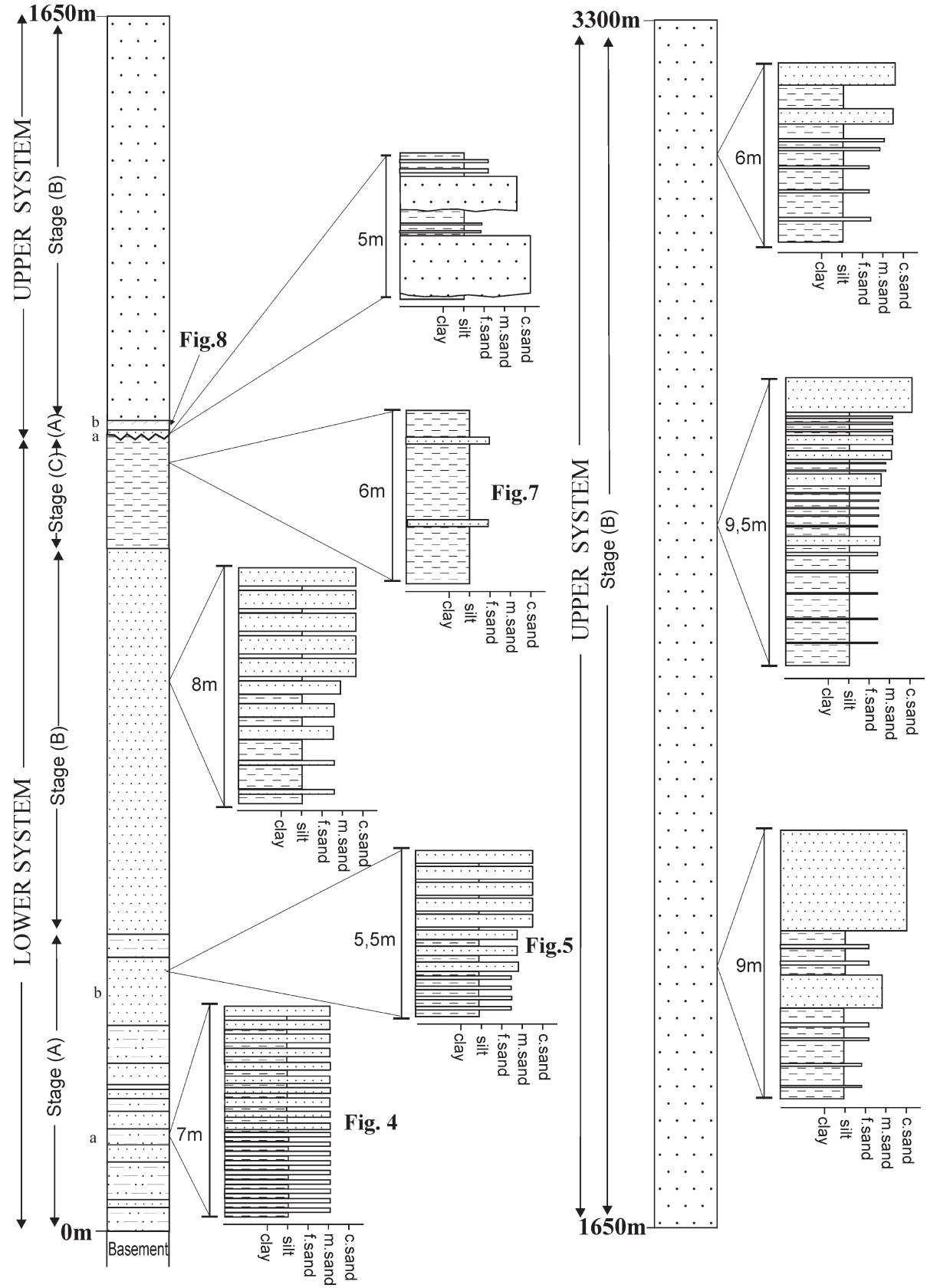


Figure 3. Geological cross-section A–A′ represented as composite stratigraphic section, 3300 m thick, exposed in the central part of the basin (Vereniki–Domolossa turbidite complex) showing the various types of turbidite cycles.

https://doi.org/10.1017/S0016756800004684 Published online by Cambridge University Press

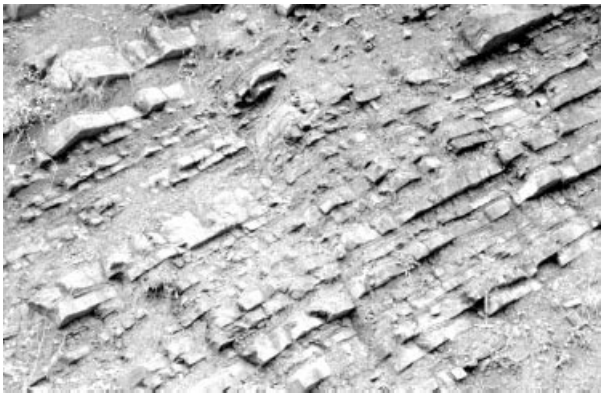


Figure 4. Cycle with 6 m thickness and s:m ratio 1:1 to 2:1, representing lobe-fringe deposits (located in Fig. 3). Length of hammer (lower right) is 33 cm.



Figure 5. Thickening- and coarsening-upward cycle with 5.5 m thickness, representing lobe deposits (located in Fig. 3).

1.5–15 cm long and the burrow fill material is sand or silt. These three types of coarsening- and thickening-upward cycles are also characterized by the presence of a mud interval (up to 3.5 m) at the beginning of each cycle, differing from the thickening- and coarsening-upward cycles of the lower turbidite system.

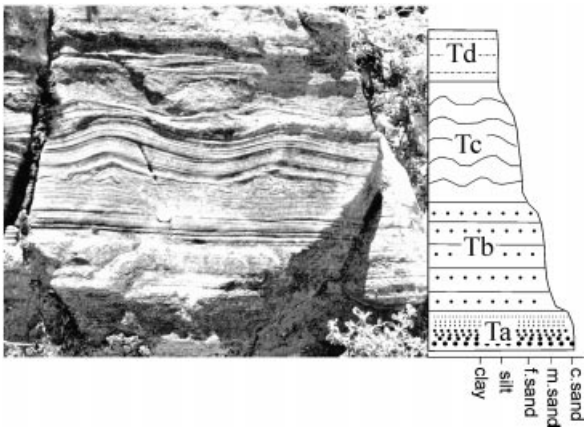


Figure 6. Partial Bouma sequence, which consists of Ta, Tb, Tc and Td Bouma intervals. Diameter of coin is 2.5 cm.

3.a.2. Interpretation

The alternations of thickening- and coarsening-upward cycles in the lower and middle turbidite stage of the lower turbidite system correspond to submarine sandstone lobe deposits using the criteria of Mutti (1977). The diagnostic features are the thick sandstone beds with thin interbedded mudstone near the upper part of each cycle and medium sandstone beds, with relatively higher mudstone ratios in the lower parts of the cycles, and the increasing upward s:m ratio from 1:1 to 6:1. The intercalations of sub-stage (a), between lobe deposits, with the s:m ratio ranging from 1:1 to 2:1 and sandstone beds in which the base of the Bouma sequence is missing, correspond to sediments deposited between the lobes and are interpreted as lobe-fringe deposits. The interpretation of these sub-stages (a and b) as lobe-fringe and lobe deposits indicates that the lower and middle turbidite stages (A and B) of the lower turbidite system represent the distal part of submarine fans and are interpreted as outer



Figure 7. Interbedded mudstone representing basin plain deposits (located in Fig. 3). Width of field of view is approximately 40 m.

https://doi.org/10.1017/S0016756800004684 Published online by Cambridge University Press



Figure 8. The slump horizon which overlies the basin plain deposits, with the chaotic bedding and the slides planes (located in Fig. 3). Length of hammer (left centre) is 33 cm.

fan deposits. The upper stage of the lower turbidite system, with the thin-bedded mudstone–siltstone alternations, indicates some pelagic or hemipelagic sedimentation and, when correlated with the lower and middle turbidite stage (outer fan), represents deposits of the more distal parts of a submarine fan, the basin plain. According to the Walker & Mutti (1973) model, the sub-stages of the lower system represent facies C (sub-stage a) and facies D (sub-stage b) of an ancient submarine fan environment. The middle turbidite stage represents cyclic alternations of lobes, deposited at the distal parts of the submarine fan and corresponds to facies D. The upper turbidite stage of the lower system, with the thin-bedded mudstones and the absence of Bouma sequence, corresponds to facies G. According to the Mutti (1985) turbidite types and the Shanmungan & Moiola (1991) types of submarine fan lobes, the interpreted lobe cycles of the lower and middle part of the lower turbidite system correspond to a type II turbidite system and they are equivalent to attached submarine fan lobes.

The lower sub-stage (a) of the lower stage of the upper turbidite system, with medium to coarse channelized thick sandstone beds, and the adjacent fine-grained thin interbedded mudstone–sandstone beds, indicates channel-fill and overbank deposits, accumulated on the inner fan. The upper sub-stage (b) of the lower stage of the upper turbidite system with chaotic bedding, slumps and slide planes is also interpreted as inner fan deposits. The coarsening- and thickening-upward cycles with thick to very thick sandstone beds and the thin interbedded mudstones, with the complete Bouma intervals, which comprise the upper stage of the upper turbidite system, are interpreted as lobe deposits, representing the outer fan. The lithology, bedding and internal features of

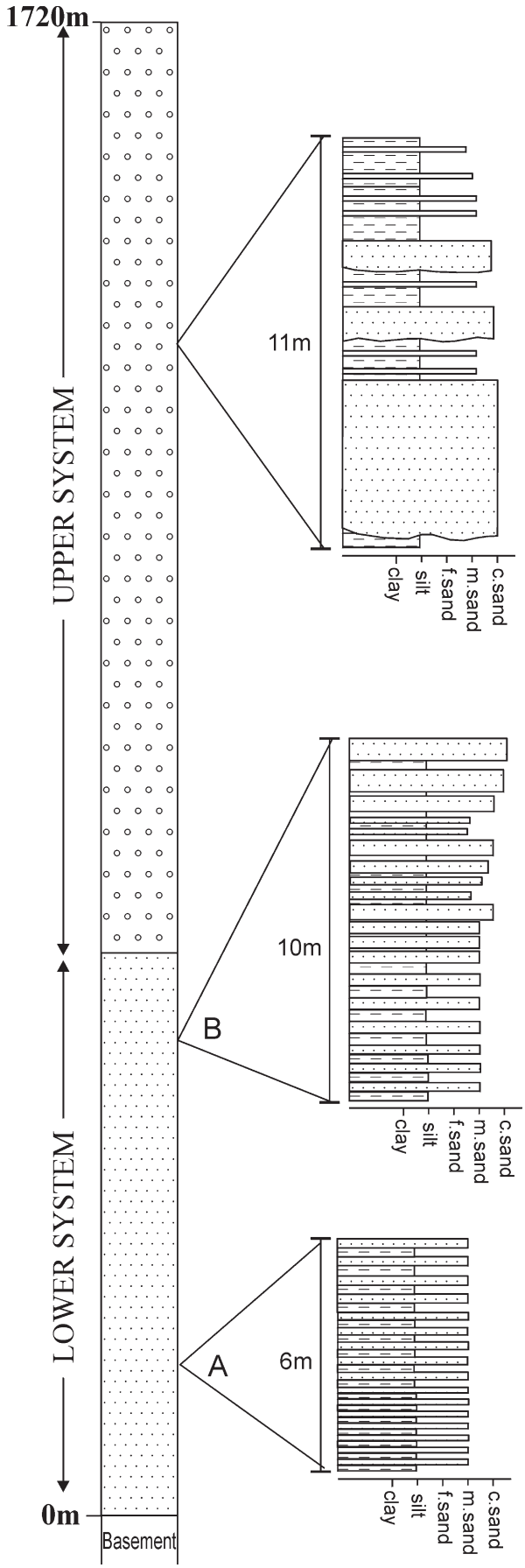


Figure 9. Geological cross-section B–B′ (Pardalitsa–Tyria turbidite complex) represented as composite stratigraphic section, up to 1720 m thick, situated in the southern part of the basin.

https://doi.org/10.1017/S0016756800004684 Published online by Cambridge University Press

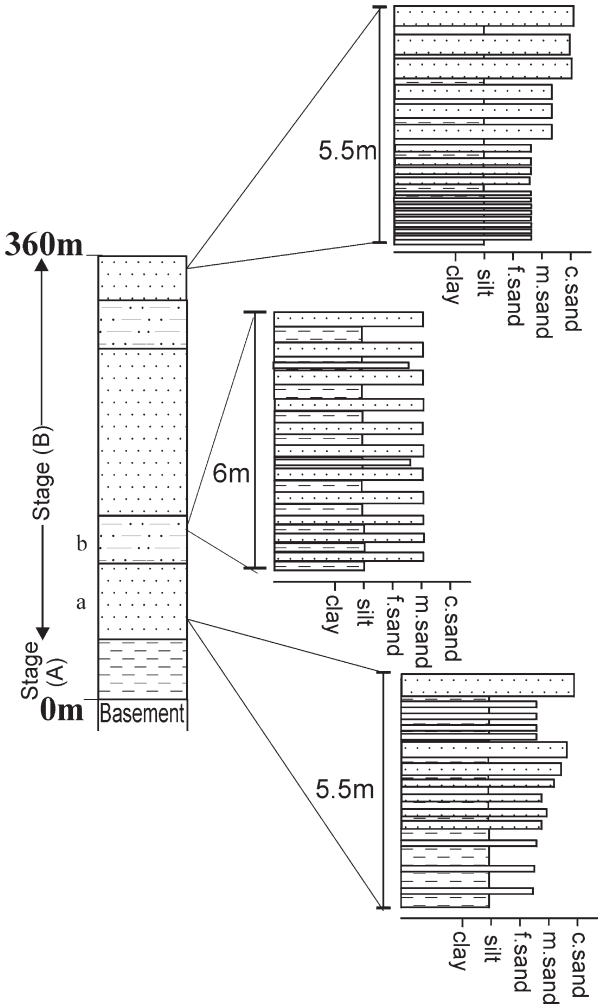


Figure 10. Geological cross-section C–C′ represented as composite stratigraphic section, up to 360 m thick, exposed in the eastern part of the basin and corresponding to Dragopsia turbidite system.

the lower and upper sub-stages in the lower stage of the upper turbidite system indicate that they correspond to facies A and B of the Walker & Mutti (1973) submarine fan facies, deposited from debris flows and turbidity currents, respectively. According to Shanmugam & Moiola (1991), the mud intervals at the base of the cycles in the upper stage of the upper system could be interpreted as a bypassing zone, between the channel-mouth and lobe deposits, representing detached lobes and corresponding to type I turbidite systems (Shanmugam & Moiola, 1991), which according to Mutti (1985) are best observed in large and elongate flysch basins of thrust belts.

3.b. Geological cross-section B–B′ (Pardalitsa–Tyria turbidite complex)

Cross-section B–B′ in the southern part of the basin has a total stratigraphic thickness up to 1720 m and it is subdivided into two turbidite systems (Fig. 9).

3.b.1. Description

Lower turbidite system: The lower system (646 m thick) is composed of two different types of cycle (A and B) which alternate (Fig. 9). Cycle (A) (up to 6 m thick) consists of thin to medium dusky yellow interbedded sandstone and blue-grey thinly interbedded mudstone beds, with s:m ratio 1:1. The thickness of sandstone beds ranges from thin bedded (10 cm), in the lower 2.5 m, to medium bedded in the upper 3.5 m (25 cm) and Bouma intervals Tbc are observed. Cycle type (B) (up to 10 m thick) consists of thin to thick interbedded dusky yellow sandstone and blue-grey mudstone beds, with s:m ratio from 1:1 to 1:2 in the lower 5 m, passing upwards to 6:1 and 8:1. The grain size of sandstone beds fluctuates from medium, in the lower 5 m, to coarse in the upper 5 m. Complete Bouma intervals are present in the upper and thicker sandstone beds, whereas Tbc intervals are observed in the sandstone beds in the lower 5 m.

Upper turbidite system: One type of repeated cycle comprises the upper system (1074 m thick) (Fig. 9). This type of cycle (up to 11 m thick) consists at the base of coarse-grained thick, channelized sandstone beds with a maximum thickness up to 4 m and a mean thickness of 1.2 m. The channelized sandstone beds pass upwards into thin to medium interbedded sandstone and mudstone beds. The sandstone beds are normally graded; in some places, the thickest sandstone beds also show amalgamation of Tabc Bouma intervals. Moreover, at the bases of thick sandstone beds, mollusc fragments are present. At the base of the sandstone beds up to 2 m thick, erosional structures such as scour marks and flutes are observed. In some places above and lateral to the sandstone channels, chaotic bedding with slide planes, slumps, and siltstone and mudstone clasts are observed. The siltstone and mudstone clasts contain aggregates of fossil fragments and coal lenses up to 10 cm thick and 30 cm wide.

3.b.2. Interpretation

Cycle type (A) of the lower turbidite system, with thin to medium bedded sandstone, thinly interbedded mudstone, and s:m ratio 1:1, is interpreted as lobe-fringe deposits. Cycle (B), with coarsening- and thickening-upward non-channelized sandstone beds, and s:m ratio of 1:1 passing upwards to 8:1, is interpreted as lobe deposits. This interpretation indicates that the lower system belongs to the distal part of a submarine fan and represents the outer fan. The bed thickness and the s:m ratio of the interpreted lobes, according to Shanmungan & Moiola (1991), indicate that the lobes are attached lobes corresponding to type II turbidite systems.

The cycles of the upper turbidite system, with fining- and thinning-upward features and channelized sandstones passing upwards to thinner and finer mud-

https://doi.org/10.1017/S0016756800004684 Published online by Cambridge University Press

stone and sandstone beds, are interpreted as channel-fill deposits. The whole upper part of the section represents the proximal part of a fan and is interpreted as the inner fan. According to Mutti & Normark's (1987) classification of the main types of channel-fill deposits, the above cycle corresponds to a depositional channel, filled with alternating sandstone and mudstone beds (b2).

3.c. Geological cross-section C–C′ (Dragopsia turbidite system)

Cross-section C–C′ in the eastern part of the basin involves turbidite sediments 360 m thick and is subdivided in two turbidite stages (Fig. 10).

3.c.1. Description

Lower turbidite stage: The lower stage (A) (48 m) conformably overlies Eocene limestone and consists of blue- grey thin to very thin interbedded mudstones and siltstones with lateral and vertical persistence and few thin bedded fine-grained sandstone intercalations (Fig. 10).

Upper turbidite stage: The upper stage (B) (321 m thick) is composed of two alternating types of turbidite sub-stage (a and b). Each type of sub-stage consists of cyclic alternations of up to 5.5–6 m thick cycles (Fig. 10).

Sub-stage (a), 63 m thick, consists of cyclic alternations up to 5.5 m thick. Each cycle consists of thickening- and coarsening-upward non-channelized calcareous sandstone beds and blue-grey thin bedded mudstones. The grain size of medium to thick sandstone beds ranges from medium to coarse. Complete Bouma intervals Tabcde are present, and at the bases of some sandstone beds sole marks are present.

Sub-stage (b), 134 m thick, consists of cycles with thin to medium fine-grained calcareous non-channelized sandstone and very thin to thin bedded mudstone beds. The contact between sandstone and mudstone beds is sharp and planar with non-erosional surfaces. The s:m ratio ranges from 1:1 to 2:1, and Tbcd Bouma intervals are present.

3.c.2. Interpretation

The lower turbidite stage (A) with the thin to very thin mudstone/siltstone beds is interpreted as basin plain deposits and corresponds to facies G of Mutti & Walker (1972).

Each coarsening- and thickening-upward cycle, with complete Bouma intervals, of sub-stage type (a) of the upper stage is interpreted as a lobe deposit. The cycle of the sub-stage type (b) of the upper stage, with thin to medium bedded sandstones/mudstones and the partial Bouma intervals, is interpreted as lobe-fringe deposits. Both types of sub-stage represent deposition on an outer fan.

4. Additional sedimentological data

4.a. Granitsopoula area

In the northern part of the Klematia–Paramythia basin, around Granitsopoula (Fig. 2), medium to very coarse-grained, thick channelized sandstone beds up to 3 m thick and 20–30 m wide and thin interbedded mudstone beds, which accumulated during Early to Middle Miocene times, are observed. Inside the sandstone bodies, coal lenses up to 10 cm thick and 20 cm wide, and fossiliferous (molluscs) resedimented clasts of mudstones are present.

In this area major and secondary channels are developed and they represent the inner fan. These channels developed near the northern termination of the Miocene basin, deposited very close to areas uplifted in the Oligocene. The source material of these channel sandstones could be from rivers crossing a very restricted delta plain and shelf area, now eroded following Miocene uplift. The overlying channel sandstones with coal lenses and fossils may represent a flooding river carrying trees as detritus and cutting a new channel across the delta plain and narrow shelf, eroding brackish molluscs.

4.b. Ardrosos–Boucovina and Agia Kyriaki fault area

In the area of Ardrosos and Boucovina villages (Fig. 2), large channelized coarse to very coarse sandstones are observed. In Ardrosos village, two stacked channels are observed, the first 110 m wide and 8 m thick, and the second one 50 m wide and 5 m thick. In Boucovina village another channel up to 90 m long and 6 m thick is also present. The channelized sandstones are overlain by medium to thick sandstone beds and thin interbedded mudstones. Except for the above major channels this whole area is characterized by secondary channels with smaller dimensions. At the bottom of these channels reworked fossils and fossil (mollusc) fragments are present.

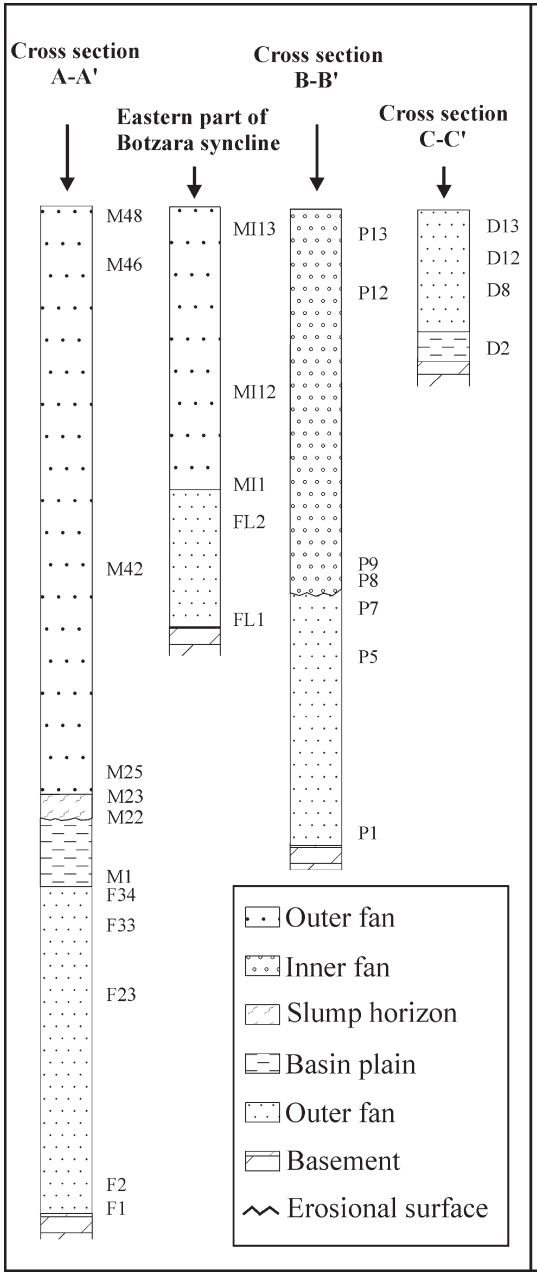
These channels represent the proximal part of the inner fan and are developed near the source of the fan which could have been a restricted shelf area. During Early Miocene to Late Miocene times, these channels were the feeder for the outer fan which developed north of the Agia Kyriaki fault (Fig. 2).

4.c. The Lippa drillhole

In the Lippa drillhole in the middle Ionian zone east of Boucovina (Fig. 2), the sedimentary succession consists of Early Oligocene deposits overlain by Miocene

https://doi.org/10.1017/S0016756800004684 Published online by Cambridge University Press

https://doi.org/10.1017/S0016756800004684 Published online by Cambridge University Press



Cross Section A-A'		
Sample	NP and NN biozones (Martini, 1971)	Nannofossil marker-species (assemblage)
M48	NN12	*Discoaster pansus, D. deflandrei, D. calculosus, D. adamanteus*
M46	NN7	*Discoaster kugleri, D. calculosus, D. deflandrei, Cyclicargolithus abisectus, Cyclicargolithus floridanus*
M42	NN7	*Discoaster kugleri, D. deflandrei, D. variabilis, Cyclicargolithus abisectus, Cyclicargolithus floridanus*
M25	NN1	*Sphenolithus conicus, Discoaster calculosus, Cyclicargolithus abisectus, Coccolithus pelagicus*
M23	NP24-25	*Dictyococcites bisectus, Helicosphaera bramlettei, H. recta, Sphenolithus celsus, Cyclicargolithus floridanus*
M22	NP24-NN2	*Sphenolithus conicus, Cyclicargolithus abisectus, Dictyococcites bisectus, Coccolithus pelagicus*
M1	NP24-NN2	*Cyclicargolithus floridanus, Cyclicargolithus abisectus, Dictyococcites bisectus, Sphenolithus conicus, Helicosphaera obliqua, Discoaster adamanteus, Coccolithus pelagicus*
F34	NP24-25	*Dictyococcites bisectus, Cyclicargolithus abisectus*
F33	NP24-25	*Dictyococcites bisectus* (acme), *Discoaster adamanteus, D. deflandrei, Coccolithus pelagicus, Reticulofenestra*
F23	NP24-25	*Helicosphaera recta, Dictyococcites bisectus, Cyclicargolithus floridanus*
F2	NP21	*Dictyococcites bisectus, Sphenolithus ciperoensis, Coccolithus pelagicus*
F1	NP21	*Ericsonia subdisticha, Reticulofenestra cf. scrippsae, Discoaster deflandrei, Sphenolithus pseudoradians, Dictyococcites bisectus*
Eastern part of Botzara syncline		
Sample	NP and NN, biozones (Martini, 1971)	Nannofossil marker-species (assemblage)
MI3	NN7	*D. deflandrei, Discoaster kugleri, D. calcaris*
MI2	NN3	*Discoaster adamanteus, D. calculosus, D. deflandrei, Dictyococcites bisectus, Helicosphaera granulata*
MI1	NP25-NN1	*Helicosphaera recta, Discoaster adamanteus, D. calculosus, D. deflandrei, Dictyococcites bisectus, Cyclicargolithus abisectus*
FL2	NP16-19	*Reticulofenestra umbilica, Chiasmolithus grandis, Discoaster tanii, D. saipanensis*
FL1	NP16-19	*Reticulofenestra umbilica, Dictyococcites bisectus, Discoaster barbadiensis,*
Cross section B-B'		
Sample	NP and NN, biozones (Martini, 1971)	Nannofossil marker-species (assemblage)
P13	NN7-8	*Discoaster kugleri, D. bollii*
P12	NN1-3	*Discoaaster adamanteus, Discoaster calculosus, D. deflandrei, Cy. abisectus*
P9	NN1	*Discoaster calculosus, D. deflandrei, Cy. abisectus*
P8	NP25-NN1	*Discoaster calculosus, D. adamanteus, D. deflandrei, Helicosphaera scissura*
P7	NP23-24	*Helicosphaera recta, Sphenolithus pseudoradians, Dictyococcites bisectus*
P5	NP20-22	*Dictyococcites bisectus, Reticulofenestra scrippsae,Sphenolithus radians, Reticulofenestra oamaruensis, R. umbilica,Helicosphaera compacta*
P1	NP17-20	*Reticulofenestra umbilica, Dictyococcites bisectus, Discoaster barbadiensis, D. Saipanensis, D. tani nodifer,E. formosa*
Cross section C-C'		
Sample	NP and NN, biozones (Martini, 1971)	Nannofossil marker-species (assemblage)
D13	NP25-NN1	*Discoaster calculosus, D. adamanteus, Helicosphaera recta, Cyclicargolithus abisectus, Dictyococcites bisectus*
D12	NP25-NN1	*Discoaster calculosus*
D8	NP17-19	*Dicoaster tanii, D. saipanenis, Helicosphaera compacta, Reticulofenestra dictyoda, R. umbilica, Dictyococcites bisectus*
D2	NP16	*Discoaster bifax, D. saipanensis, Chiasmolithus modestus, C. solitus, C. modestus, Nannotetrina fulgens*

Figure 11. Stratigraphic distribution of calcareous nannofossil biozones and nannofossil marker-species assemblage of the three studied cross-sections and the eastern part of Botzara syncline based on Martini (1971) biozones.

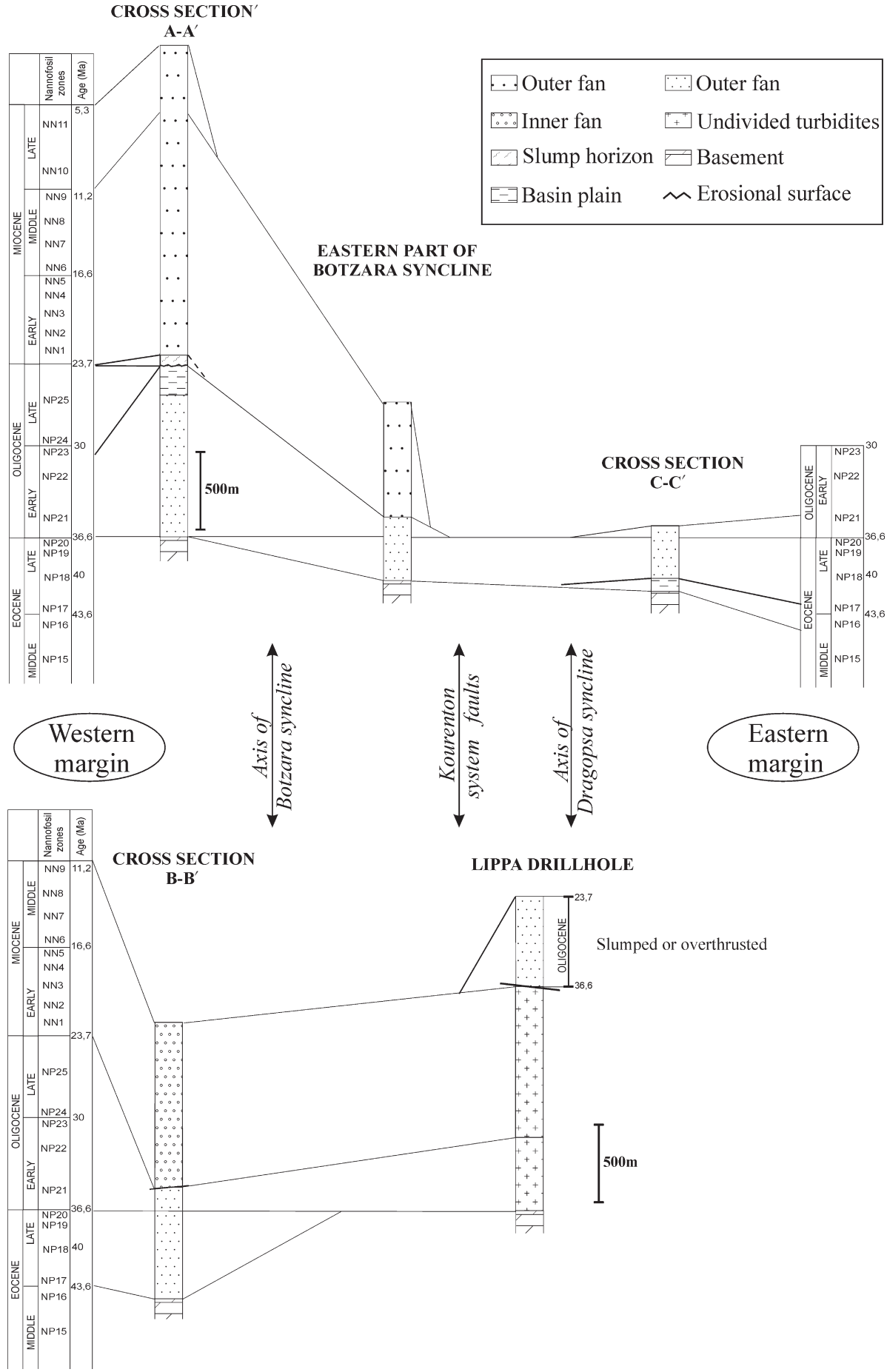


Figure 12. For legend see facing page.

https://doi.org/10.1017/S0016756800004684 Published online by Cambridge University Press

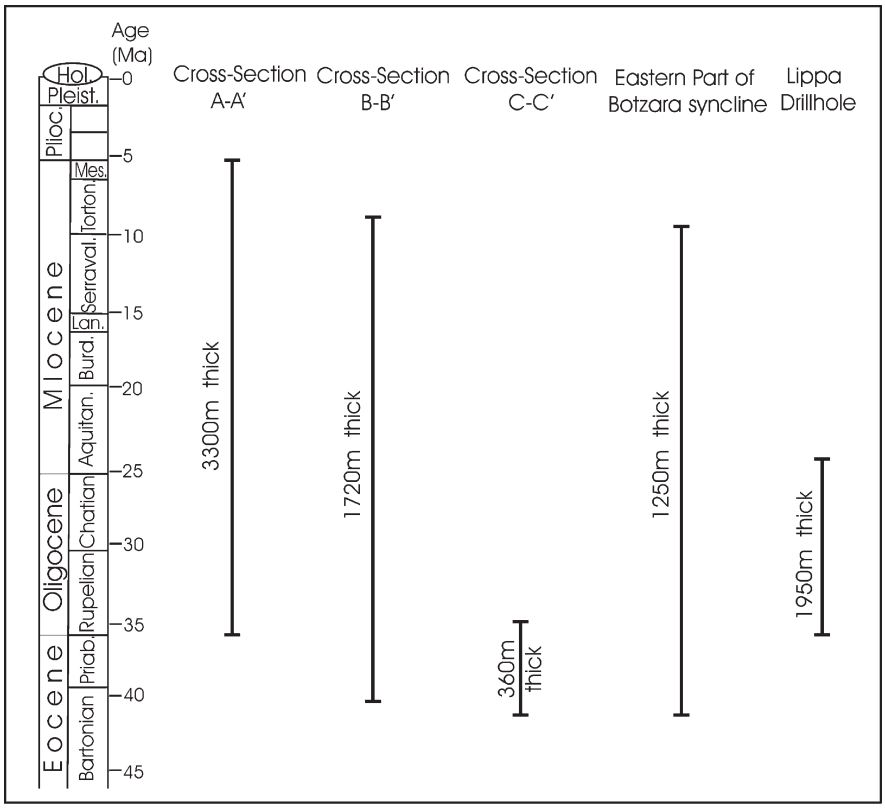


Figure 13. A simple time section, presenting the places where sedimentation was taken place along the Klematia–Paramythia basin, from Middle Eocene to Late Miocene.

deposits. In the upper part of the drillhole, Oligocene lobe facies are present, probably slumped or overthrust on the Miocene (Fig. 12) (data obtained from the Public Petroleum Corporation of Greece – Exploration and Exploitation of Hydrocarbons S.A.).

5. Palaeogeographic evolution

5.a. Tectonic elements of the Pindos foreland basin

Five main thrusts influenced the evolution of Pindos foreland basin. The Pindos and Ionian thrusts are the major thrusts situated at the eastern and western ends of the Pindos foreland basin, respectively. As a result of Pindos thrust activity, the Pindos foredeep was formed during the Middle Eocene (IGSR & IFP, 1966). Ionian thrust activity transformed the foreland basin into a piggy-back basin or thrust sheet-top, northwards (studied area) during Late Oligocene times, according to Wilspaar (1995), and southwards (Zakynthos area) during the Early Pliocene, according to Zelilidis *et al.* (1998). This diachronous deformation of the Ionian thrust (Zelilidis *et al.* 1998) probably results from the presence of the Hellenic trench west of Zakynthos, the lack of a continental block west of the Pre-Apulian zone and the presence of Triassic evaporites (Underhill, 1988, 1989).

The Gavrovo, internal Ionian and middle Ionian thrusts (Fig. 1) are minor thrusts situated internally within the Pindos foreland basin. Movement on these faults during the Early Oligocene caused the foreland basin to be modified into a complex type of foreland basin. The Gavrovo thrust marks the western margins of the Gavrovo zone, whereas the internal and middle Ionian thrusts subdivided the Ionian zone into three sub-zones: internal, middle (the area of this study) and external.

Moreover, strike-slip faults like the Agia Kyriaki and Kourenton faults influenced depositional environments and basin evolution. The Agia Kyriaki fault runs perpendicular to major thrusting, and sedimentation in the Gavrovo zone during Late Eocene times (according to the maps IGSR & IFP, 1966) terminated on this fault and was restricted southwards, indicating

Figure 12. Stratigraphic correlation between the exposed geological cross-sections A–A', B–B', C–C', the eastern part of Botzara syncline and the Lippa drillhole, based on age determination and the described turbidite sub-environments. The age determination is based on standard nannofossil biozones of Martini (1971) and the Lippa drillhole geological data provided by the Public Petroleum Corporation of Greece (Exploration and Exploitation of Hydrocarbons S.A.).

https://doi.org/10.1017/S0016756800004684 Published online by Cambridge University Press

that this strike-slip fault acted as a tear fault during this period. This E–W-trending strike-slip fault (Figs 1, 2) affected the deposition of the Lias–Eocene carbonate and siliceous rocks (IGSR & IFP, 1966) and the Oligocene–Miocene turbidites (Pavlides, 1996; Boccaletti *et al.* 1997). The Kourenton fault, which runs parallel to major thrusting, seems to have a transpressional character, according to King, Strudy & Whitney (1993), while it has been interpreted as a backthrust by the IGSR & IFP (1966).

5.b. Stratigraphic elements of the studied basin

The age determination of the studied turbidite deposits (Fig. 11) was based on calcareous nannofossil biozones NP and NN of Martini (1971). Based on these nannofossil determinations, the age of the sediments in the studied basin showed that Middle to Late Eocene deposits could be recognized: (1) in the western margins of the Botzara syncline and south of the Agia Kyriaki strike-slip fault (section B–B′) within lobe deposits, (2) in the eastern margins of the Botzara syncline but north of the Agia Kyriaki fault (eastern part of Botzara syncline) within lobe deposits and (3) in the Dragopsia syncline and within basin plain deposits (cross-section C–C′) (Figs 12, 13).

Sedimentation in the Botzara syncline was continuous until Late Miocene times (cross-section A–A′) and until Middle Miocene times in the Dragopsia syncline (cross-section C–C′) (Fig. 12).

The age of the slump horizons based on the age of the underlying and overlying deposits shows that the slumping in section A–A′ probably took place after the latest Oligocene, but occurred in the Lippa drill hole after Middle Miocene times (Fig. 12).

5.c. Palaeocurrent data

The palaeoflow trends during the first tectonic phase (Middle Eocene–Late Oligocene) have been estimated from the sole marks at the base of sandstone beds. Moreover, channel sandstones suggest E–W and ENE–WSW trends (Fig. 14a). The projection in rose diagrams of the mean palaeocurrent direction from sole marks from 42 localities indicates an ENE–WSW palaeoflow direction (Fig. 14b). At every locality 5 to 13 measurements were taken. The palaeocurrent data from Middle Eocene to Late Oligocene deposits show that the development of the submarine fans was almost parallel to the westward progradation of the external Hellenides.

The palaeoflow trends during the second tectonic phase (Late Oligocene–Late Miocene) have been estimated from channels, observed in the inner fan and from the mean palaeocurrent direction from sole marks from 41 localities (up to 13 measurements at every locality were taken). The projection in rose diagrams of the sole marks shows two major palaeoflow directions (Fig. 14b), which have already observed from channels (NNW–SSE and WSW–WNW).

5.d. Facies distribution

According to Aubouin (1965) and IGSR & IFP (1966), the Gavrovo zone (part of the Pindos foreland) was a ridge during Early Eocene times, whereas the Ionian zone was a trough. Both areas were characterized by carbonate sedimentation. As a result of Pindos thrust activity the Gavrovo ridge and Ionian basin changed to a foredeep.

From Middle Eocene to Late Miocene times, the clastic deposits of the Klematia–Paramythia basin accumulated in two different basin configurations within the middle Ionian zone (Fig. 15). The first configuration accumulated during Middle Eocene–Late Oligocene times, when sediments covered the whole basin and were deposited conformably over the Eocene limestone basement (Fig. 15a). The studied area generally corresponds during this phase to the outer parts of the Pindos foredeep. The second configuration was formed during latest Oligocene–Late Miocene times (Fig. 15b), when sediments were restricted basinwards and deposited unconformably over the Middle Eocene–Late Oligocene sediments.

In the first basin configuration (Middle Eocene–Late Oligocene), three facies associations were recognized (Fig. 12): (a) in the eastern part of the basin, Middle Eocene basin plain deposits passing upwards to Late Eocene–Late Oligocene outer fan sandstone lobes (cross-section C–C′); (b) in the western part of the basin, Early Oligocene outer fan sandstone lobes passing upwards to Middle Oligocene–Late Oligocene basin plain deposits (western part of cross-section A–A′); and (c) Late Eocene–Late Oligocene outer fan sandstone lobes were deposited in the western part of cross-section B–B′ where basin plain deposits are absent.

This first basin configuration is related to the Pindos thrust activity which resulted in formation of a foreland basin where submarine fan deposits accumulated (Fig. 15a). In the Middle Eocene–Late Oligocene, adjacent to the thrust front, coarse-grained sediments were deposited, representing the inner fan and belonging now to the Gavrovo and internal Ionian zones. Basinwards, with westward progradation, outer fan and basin plain deposits were formed, which now in part belong to the middle Ionian zone.

King, Strudy & Whitney (1993) interpreted the Agia Kyriaki fault as a strike-slip fault. Mapping the subenvironments near the fault, inner fan deposits are present (Fig. 2) such as in section B–B′, suggesting a relatively steep sea floor. The activity of this fault explains the greater development of inner fan deposits in the southern part compared with the northern part of the study basin. The existence of a steep area of the north Agia Kyriaki fault can be explained if the fault

https://doi.org/10.1017/S0016756800004684 Published online by Cambridge University Press

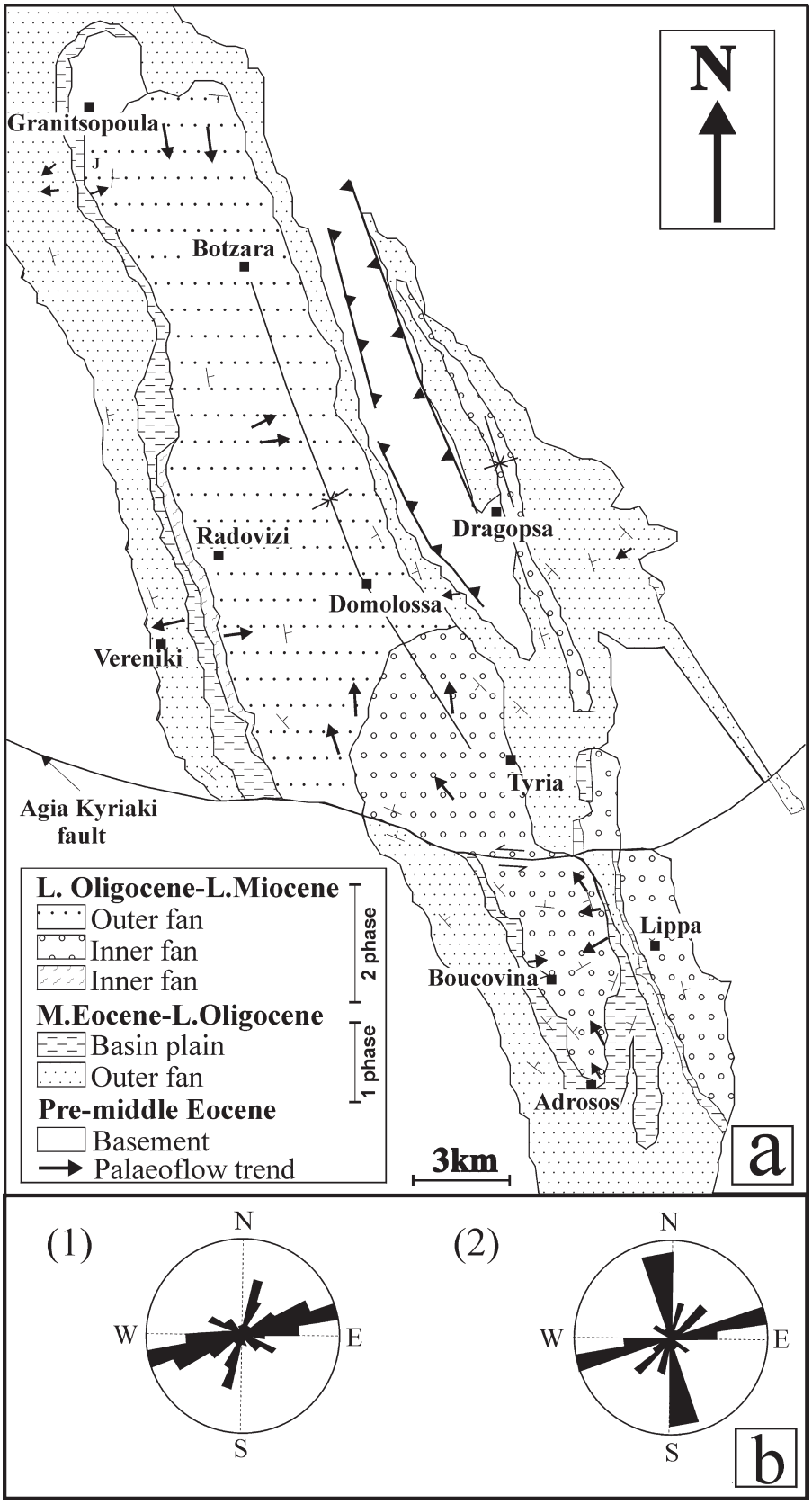


Figure 14. (a) Sub-environment distributions and palaeoflow trends of the Klematia–Paramythia basin turbidite deposits (after Avramidis & Kontopoulos, 1998). (b) Rose diagrams of mean palaeocurrent direction from sole marks from 42 localities of the first (1) and 41 localities of the second tectonic phase (2) (up to 13 measurements at every locality were taken).

https://doi.org/10.1017/S0016756800004684 Published online by Cambridge University Press

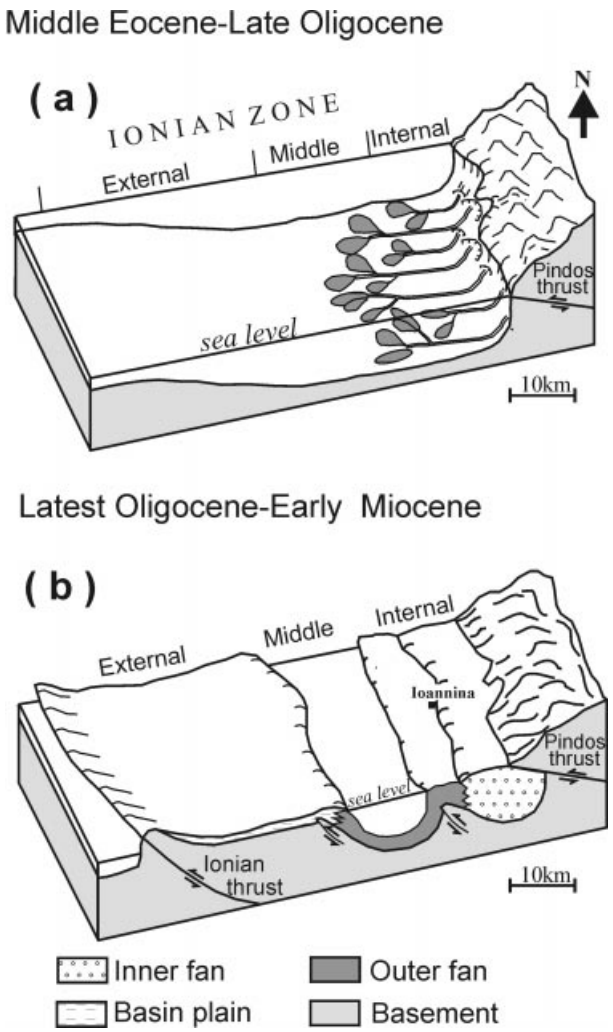


Figure 15. Block diagram modelling the Ionian zone: (a) during Middle Eocene–Late Oligocene (first tectonic phase), where Ionian zone was a foreland basin and in the middle Ionian zone outer fan deposits accumulated, (b) during latest Oligocene–Early Miocene (second tectonic phase), where the Ionian zone began to act as a complex type foreland basin.

has a normal character. We therefore suggest that the Agia Kyriaki fault is a transtensional strike-slip fault, which influenced the palaeorelief in the southern part of the basin, providing a submarine fan with suitable conditions to develop inner fan deposits.

The alternation of facies associations in relation to the age of these deposits probably indicates four evolutionary stages with fluctuation of basin width (Fig. 12):

(1) During the Middle Eocene, the foredeep was narrow because basin plain deposits accumulated in the eastern part of the studied area. Outer fan lobes were probably deposited east of the studied basin, in the Ioannina area (Fig. 1).

(2) During the Late Eocene, the basin was wider because outer fan sandstone lobes accumulated in the eastern part of the major basin with basin plain deposits developed in a westward direction; these basin plain deposits are now probably buried under latest Oligocene–late Miocene deposits. The presence in this stage of sediments at the western margins of the basin south of the Agia Kyriaki fault suggests that a small depression formed in this area due to strike-slip fault activity. This depression did not extend as far as the Lippa drillhole, where Eocene deposits are absent.

(3) During the Early Oligocene, the foredeep had its maximum width because only outer fan sandstone lobes accumulated in the studied area. Basin plain deposits during this stage probably accumulated to the west in the external Ionian zone.

(4) During the Middle to Late Oligocene, the foredeep became restricted again because basin plain deposits accumulated in the western parts of the studied basin and outer fan sandstone lobes in the eastern part.

A latest Oligocene slump horizon (cross-section A–A′) (Figs 3, 12) was developed over Middle Eocene–Late Oligocene deposits only in the western margins of the basin and north of the Agia Kyriaki fault. This slump horizon marks the onset of the second basin configuration from latest Oligocene to Late Miocene, which is related to the subdivision of the Ionian zone at that time into the internal, middle and external sub-basins (Fig. 15b). This subdivision resulted from internal Ionian zone thrusting, whereby the internal Ionian zone which was situated on its hangingwall became emergent. Pindos thrust activity either stopped or decreased considerably. In consequence, an elongated basin was formed parallel to the thrust direction (NNW–SSE) and situated in the western part of the middle Ionian zone. This may correspond to the beginning of minor thrusting on the Ionian thrust west of the Ionian zone and a decrease in the activity of the Pindos thrust. At this time, the Ionian zone changed from a foredeep to a complex type foreland basin.

The main sedimentation was restricted to the western part of the middle Ionian zone (Botzara syncline). In the other areas either the sedimentation stopped or the sediments which were very thin following emersion were eroded (Dragopsia syncline). The distribution of sub-environments was different along and across the basin axis. There were no inner fan deposits in the eastern parts of the Botzara syncline, only in the western parts and near the northern and southern termination (Fig. 2). Miocene deposits are absent in the eastern part of the middle Ionian zone (around Ioannina area) and also are absent in the external and internal Ionian zones (Fig. 1), but resedimented shelf deposits of Miocene age accumulated at the northern and southern ends of the Botzara syncline.

In this model of a complex type of foreland basin, we propose that:

(1) the Pindos thrust was still active during latest Oligocene times, but its activity was strongly reduced,

https://doi.org/10.1017/S0016756800004684 Published online by Cambridge University Press

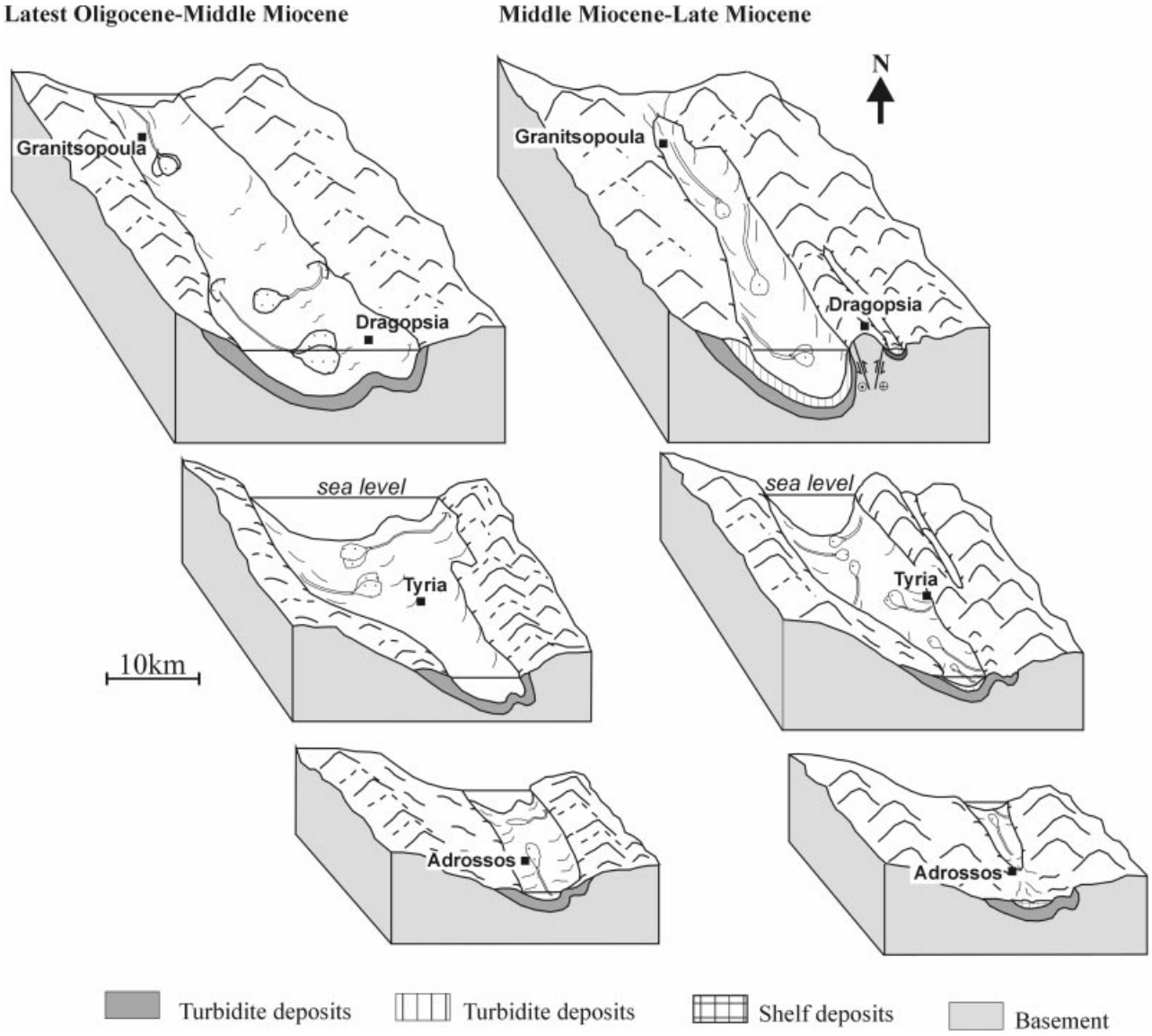


Figure 16. Block diagram modelling the Klematia–Paramythia basin deposits, during latest Oligocene to Late Miocene (second tectonic phase), after the Ionian zone subdivision and while the Ionian zone was acting as a complex type foreland basin.

(2) internal thrusting during the latest Oligocene subdivided the Ionian zone into three sub-basins, and

(3) the Ionian thrust began its activity at this time (latest Oligocene–Early Miocene), and this activity is recorded by uplift of its hangingwall (external Ionian zone), where Miocene deposits either were not deposited or were very thin and later eroded.

The absence of sedimentation in the eastern part of the middle Ionian zone might be the result of a flower-like structure within the middle Ionian zone, as proposed by King, Strudy & Whitney (1993) on the basis of a flower-like structure between the Botzara and Dragopsia synclines (Fig. 16). Whatever the tectonic origin, the basin became emergent and the overlying sediments were eroded, with the inner fan extending eastwards in the Dragopsia syncline.

The inner fan deposits at the southern and northern ends of the studied basin, containing resedimented shelf deposits, indicate that strike-slip fault activity and the consequent uplift in these areas (King, Strudy & Whitney, 1993) took place synchronously with the basin evolution and influenced the basin configuration. Thus, as a result of transpressive uplift, the elongated latest Oligocene basin (from Albania to Amvrakikos Gulf) was separated into three sub-basins, the central one of which was focused on in this study (Fig. 1). In the uplifted areas shelf environments were formed first, then subsequently emerged and were eroded (Fig. 16).

6. Conclusions

The Ionian and Gavrovo zones formed a foreland basin where submarine fans accumulated from Middle

https://doi.org/10.1017/S0016756800004684 Published online by Cambridge University Press

Eocene to Late Oligocene times. During this time in the Klematia–Paramythia basin outer fan (sandstone lobe and lobe-fringe) and basin plain deposits were formed. The evolution of the foreland basin was influenced by the major activity on the Pindos thrust.

During latest Oligocene to Early Miocene times, the foreland basin became subdivided into three sub-basins: internal, middle and external, and sedimentation continued only in the middle sub-basin. In this middle sub-basin three elongated and restricted marine environments developed; the Klematia–Paramythia basin is the central sub-basin of the middle Ionian zone.

Extensive shelf environments were formed at the northern and southern terminations of this sub-basin, connecting thus with the other two analogous sub-basins. In the rest of the sub-basin, submarine fans were deposited, characterized by inner fan deposits (channel-fill) in the southern and northern areas of the basin and slumps at its western margins. Strike-slip fault activity during this period at the southern end of the basin influenced the inner fan environment, producing an extensive unstable area.

Acknowledgements. The authors would like to thank the editors of the journal and two anonymous reviewers for their constructive comments and the Public Petroleum Corporation of Greece (Exploration and Exploitation of Hydrocarbons S.A.) for the data from the Lippa drillhole. The first author is deeply indebted the Greek National Foundation of Scholarships for the financial support during his Ph.D. study, of which the present paper is a part.

References

AUBOUIN, J. 1965. *Geosynclines*. Amsterdam: Elsevier, 350 pp.

ALEXANDER, J., NICHOLS, G. J. & LEIGH, S. 1990. The origins of marine conglomerates in the Pindus foreland basin, Greece. *Sedimentary Geology* **66**, 243–54.

AVRAMIDIS, P. & KONTOPOULOS, N. 1998. Hydraulic determination and palaeoflow trends of turbidite deposits in Klematia–Paramythia basin. *Bulletin Geological Society of Greece* **XXXII** (2), 299–307.

AVRAMIDIS, P. & ZELILIDIS, A. 1998. Two different submarine fan lobe types and their relationship to basin evolution; Implication to hydrocarbon reservoirs, western Greece. *Bulletin Geological Society of Greece* **XXXII** (2), 165–73.

BELLAS, S. M. 1997. Calcareous nannofossils of the Tertiary flysch (Post Eocene to Early Miocene) of the Ionian zone in Epirus NW-Greece: Taxonomy and Biostratigraphical correlations. *Berliner Geowissenschaftliche Abhandlungen* **22**, 173 pp.

BOCCALETTI, M., CAPUTO, R., MOUNTRAKIS, D., PAVLIDES, S. & ZOUROS, N. 1997. Paleoseismicity of the Souli fault, Epirus, Western Greece. *Journal Geodynamics* **24**, 117–27.

BOIANO, U. 1997. Anatomy of a siliciclastic turbidite basin: the Gorgoglione flysch, Upper Miocene, southern Italy: physical stratigraphy, sedimentology and sequence–stratigraphic framework. *Sedimentary Geology* **107**, 231–62.

BOUMA, A. H. 2000. Coarse-grained and fine-grained turbidite systems as end member models: applicability and dangers. *Marine and Petroleum Geology* **17**, 137–43.

BOUMA, A. H. 1962. *The sedimentology of some flysch deposits: a graphic approach to facies interpretation*. Amsterdam: Elsevier, 168 pp.

BRITISH PETROLEUM CO. LTD. (B.P.) 1971. *The geological results of petroleum exploration in western Greece.* Institute for Geology and Subsurface Research, Special report no. 10, Athens.

BROOKS, M., CLEWS, J. E., MELIS, N. S. & UNDERHILL, J. R. 1988. Structural development of Neogene basins in Western Greece. *Basin Research* **1**, 129–38.

CLEWS, J. 1989. Structural controls on basin evolution: Neogene to Quaternary of the Ionian zone of western Greece. *Journal of the Geological Society, London* **146**, 447–57.

DERCOURT, J. & THIEBAULT, F. 1979. Creation and evolution of the northern margin of the Mesogean ocean between Africa and Apulia in the Peloponnesus (Greece). *Proceedings VI Colloquium on the Geology of the Aegean region, Athens* **3**, 1313–32.

FAUPL, P., PAVLOPOULOS, A. & MIGIROS, G. 1998. On the provenance of flysch deposits in the External Hellenides of mainland Greece: results from heavy mineral studies. *Geological Magazine* **135**, 412–42.

FLEURY, J. J. 1980. Les zones de Gavrovo-Tripolitza et du Pinde-Olonus (Grèce occidentale et Péloponnese du Nord): evolution d'une plateforme et d'une bassin dans leur cadre alpin. *Société Géologique du Nord* **4**, 1–651.

GHIBAUDO, G. 1992. Subaqueous sediment gravity flow deposits: practical criteria for their field description and classification. *Sedimentology* **39**, 423–54.

HISCOTT, R. N., PICKERING, K. T. & BEEDEN, D. R. 1986. Progressive filling of a confined Middle Ordovician foreland basin associated with the Taconic Orogeny, Quebec, Canada. In *Foreland basins* (eds P. A. Allen and P. Homewood), pp. 309–26. International Association of Sedimentologists, Special Publication no. 8.

INSTITUTE FOR GEOLOGY SUBSURFACE RESEARCH OF GREECE & INSTITUTE FRANCAIS DE PÉTROLE. 1966. *Etude geologique de l'Epire.* Paris: Technip, 306 pp.

JONES, G., DEWEVER, P. & ROBERTSON, A. H. F. 1992. Significance of radiolarian age data to the Mesozoic tectonic and sedimentary evolution of the northern Pindos Mountains, Greece. *Geological Magazine* **129**, 385–400.

KING, G., STRUDY, D. & WHITNEY, J. 1993. The landscape geometry and active tectonics of northwest Greece. *Geological Society of America Bulletin* **105**, 137–61.

MARTINI, E. 1971. Standard Tertiary and Quaternary calcareous nannoplankton zonation. *2nd International Conference on Planktonic Microfossils, Roma* **2**, 739–85.

MUTTI, E. 1977. Distinctive thin-bedded turbidite facies and related depositional environments in the Eocene Hecho Group (south-central Pyrenees, Spain). *Sedimentology* **24**, 107–31.

MUTTI, E. 1979. Turbidites et cones sous-margins profonds. In *Sédimentation Détrique Fluviatile, Littorale et marine* (ed. P. Homewood), pp. 352–419. Institute Geologie Université de Fribourg, Fribourg.

MUTTI, E. 1985. Turbidite systems and their relations to depositional sequences. In *Provenance of arenites: Dordrecht* (ed. G. G. Zuffa), pp. 65–93. D. Reidel Publishing Company.

MUTTI, E. & NORMARK, W. R. 1987. Comparing examples

https://doi.org/10.1017/S0016756800004684 Published online by Cambridge University Press

of modern and ancient turbidite systems: Problems and concepts. In *Marine clastic sedimentology: concepts and case studies* (eds J. K. Leggett and G. G. Zuffa), pp. 1–37. London: Graham and Trotman.

Mutti, E. & Ricci Lucchi, F. 1972. Turbidites of the northern Apennines; introduction to facies analysis. (Translated into English by T. H. Nilsen, 1978). *International Geological Review* **20**, 125–66.

Mutti, E. & Ricci Lucchi, F. 1975. Turbidite facies and facies associations. In *Examples of turbidite facies and facies associations from selected formations of the northern Apennines* (I.A.S. fieldtrip guidebook A-11), 21–36. International Sedimentological Congress IX.

Nelson, C. H. & Nilsen, T. H. 1984. Modern and ancient deep-sea fan sedimentation. *Society of Economic Paleontologists and Mineralogists, Short course* **14**, 404.

Normark, W. R. 1970. Growth patterns of deep sea fans. *American Association of Petroleum Geologists Bulletin* **54**, 2170–95.

Ori, G. G., Roveri, M. & Vannoni, F. 1986. Plio-Pleistocene sedimentation in the Apenninic–Adriatic foredeep (Central Adriatic Sea, Italy). In *Foreland basins* (eds P. A. Allen and P. Homewood), pp. 183–98. International Association of Sedimentologists, Special Publication no. 8.

Pavlides, S. 1996. First palaeoseismological results from Greece. *Annali di Geofisica* **XXXIX** (3), 545–55.

Pickering, K. T., Hiscott, R. N. & Hein, F. J. 1989. *Deep marine environments*. London: Unwin Hyman, 352 pp.

Pickering, K. T., Stow, D., Watson, M. & Hiscott, R. N. 1986. Deep-water facies processes and models: a review and classification scheme for modern and ancient sediments. *Earth-Science Review* **23**, 75–174.

Piper, D. J. W., Panagos, A. G. & Pe, G. G. 1978. Conglomeratic Miocene flysch, western Greece. *Journal of Sedimentary Petrology* **48**, 117–26.

Reading, H. G. & Richards, M. 1994. Turbidite systems in deep water basin margins classified by grain size and feeder system. *American Association of Petroleum Geologists Bulletin* **78**, 792–822.

Ricci Lucchi, F. 1975. Depositional cycles in two turbidite formations of northern Apennines (Italy). *Journal of Sedimentary Petrology* **45**, 3–43.

Ricci Lucchi, F. 1986. The Oligocene to recent foreland basins of the northern Apennines. In *Foreland basins* (eds P. A. Allen and P. Homewood), pp. 105–40. International Association of Sedimentologists, Special Publication no. 8.

Robertson, A. H. F., Clift, P. D., Degnan, P. J. & Jones, G. 1991. Palaeogeographic and palaeotectonic evolution of the Eastern Mediterranean Neotethys. *Palaeogeography, Palaeoclimatology, Palaeoecology* **87**, 289–343.

Shanmugam, G. 1997. The Bouma sequence and the turbidite mind set. *Earth-Science Review* **42**, 201–29.

Shanmugam, G. 2000. 50 years of the turbidite paradigm (1950s–1990s): deep-water processes and facies models – a critical perspective. *Marine and Petroleum Geology* **17**, 285–342.

Shanmugam, G., Damuth, J. E. & Moiola, R. J. 1985. Is the turbidite facies association scheme valid for interpreting ancient submarine fan environments? *Geology* **13**, 234–7.

Shanmugam, G. & Moiola, R. J. 1985. Submarine fan models: Problems and solutions. In *Submarine fans and related turbidite systems* (eds A. H. Bouma, W. R. Normark and N. E. Barnes), pp. 29–34. New York: Springer-Verlag.

Shanmugam, G. & Moiola, R. J. 1988. Submarine fans: characteristics, models, classification and reservoir potential. *Earth-Science Review* **24**, 383–428.

Shanmugam, G. & Moiola, R. J. 1991. Types of submarine fan lobes: Models and implications. *American Association of Petroleum Geologists Bulletin* **75**, 156–79.

Stow, D. A. V. & Mayall, M. 2000. Deep-water sedimentary systems: New models for the 21st century. *Marine and Petroleum Geology* **17**, 125–35.

Stow, D. A. V., Reading, H. G. & Collinson, J. D. 1996. Deep Seas. In *Sedimentary Environments* (ed. H. G. Reading), pp. 395–453. New York: Elsevier.

Underhill, J. R. 1988. Triassic evaporites and Plio-Quaternary diapirism, western Greece. *Journal of the Geological Society, London* **145**, 269–82.

Underhill, J. R. 1989. Late Cenozoic deformation of the Hellenide foreland, western Greece. *Geological Society of America Bulletin* **101**, 613–34.

Walker, R. G. & Mutti, E. 1973. Turbidite facies and facies associations. In *Turbidites and Deep-Water Sedimentation* (eds G. V. Middleton and A. H. Bouma), pp. 119–57. Pacific Section, Society of Economic Paleontologists and Mineralogists, Los Angeles, California.

Walker, R. G. 1978. Deep water sandstone facies and ancient submarine fans: models for exploration for stratigraphic traps. *American Association of Petroleum Geologists Bulletin* **62**, 932–66.

Weimer, P. & Link, M. H. 1991. Global petroleum occurrences in submarine fans and turbidite systems. In *Seismic facies and sedimentary processes of submarine fans and turbidite systems* (eds P. Weimer and M. H. Link), pp. 9–67. New York: Springer Verlag.

Wilpshaar, M. 1995. Applicability of dinoflagellate cyst stratigraphy to the analyses of passive and active tectonic settings. *Geologica Ultraiectina* **134**, 132 pp.

Zelilidis, A., Kontopoulos, N., Avramidis, P. & Piper, D. J. W. 1998. Tectonic and sedimentological evolution of the Pliocene–Quaternary basins of Zakynthos island, Greece: Case study of the transition from compressional to extensional tectonics. *Basin Research* **10**, 393–408.

https://doi.org/10.1017/S0016756800004684 Published online by Cambridge University Press